ISSN 1674-1056
http://cpb.iphy.ac.cn
http://iopscience.iop.org/cpb
中国物理 B
Chinese Physics
中国物理 Chinese Physics B

Unitary transformation of general nonoverlapping-image multimode interference couplers with any input and output ports

Ze-Zheng Li(李泽正)[1,2], Wei-Hua Han(韩伟华)[2], Zhi-Yong Li(李智勇)[2]
Citation: Chin. Phys. B . 2020, 29(1): 014206 . **doi:** 10.1088/1674-1056/ab5783
Journal homepage: http://cpb.iphy.ac.cn; http://iopscience.iop.org/cpb

What follows is a list of articles you may be interested in

Compact and high-efficient wavelength demultiplexing coupler based on high-index dielectric nanoantennas

Jingfeng Tan(谭敬丰), Hua Pang(庞画), Fengkai Meng(孟凤凯), Jin Jiang(蒋进)
Chin. Phys. B . 2018, 27(9): 094217 . **doi:** 10.1088/1674-1056/27/9/094217

Graphene integrated photodetectors and opto-electronic devices–a review

Xiaomu Wang(王肖沐), Xuetao Gan(甘雪涛)
Chin. Phys. B . 2017, 26(3): 034203 . **doi:** 10.1088/1674-1056/26/3/034203

Crosstalk analysis of silicon-on-insulator nanowire-arrayed waveguide grating

Kai-Li Li(李凯丽), Jun-Ming An(安俊明), Jia-Shun Zhang(张家顺), Yue Wang(王玥), Liang-Liang Wang(王亮亮), Jian-Guang Li(李建光), Yuan-Da Wu(吴远大), Xiao-Jie Yin(尹小杰), Xiong-Wei Hu(胡雄伟)
Chin. Phys. B . 2016, 25(12): 124209 . **doi:** 10.1088/1674-1056/25/12/124209

Turbulence mitigation scheme based on multiple-user detection in an orbital-angular-momentum multiplexed system

Li Zou(邹丽), Le Wang(王乐), Sheng-Mei Zhao(赵生妹), Han-Wu Chen(陈汉武)
Chin. Phys. B . 2016, 25(11): 114215 . **doi:** 10.1088/1674-1056/25/11/114215

X-ray communication based simultaneous communication and ranging

Song Shi-Bin, Xu Lu-Ping, Zhang Hua, Gao Na
Chin. Phys. B . 2015, 24(9): 094215 . **doi:** 10.1088/1674-1056/24/9/094215

Unitary transformation of general nonoverlapping-image multimode interference couplers with any input and output ports*

Ze-Zheng Li(李泽正)[1,2], Wei-Hua Han(韩伟华)[2], and Zhi-Yong Li(李智勇)[2,†]

[1] College of Materials Science and Opto-Electronic Technology, University of Chinese Academy of Sciences, Chinese Academy of Sciences, Beijing 100049, China

[2] State Key Laboratory on Integrated Optoelectronics, Institute of Semiconductors, Chinese Academy of Sciences, Beijing 100083, China

(Received 25 August 2019; revised manuscript received 23 September 2019; accepted manuscript online 14 November 2019)

An explanation of optical unitary transformation is presented for general nonoverlapping-image multimode interference (MMI) couplers with any number of input and output ports. The light transformation in the MMI coupler can be considered as an optical field matrix acting on an input light column vector. We investigate the general phase principle of output light image. The complete proof of nonoverlapping-image MMI coupler's optical unitarity along with the phase analysis of matrix element is provided. Based on a two-dimensional finite-difference time-domain (2D-FDTD) simulation, the unitary transformation is obtained for a 4×4 nonoverlapping-image MMI coupler within a deviation of 4×10^{-2} for orthogonal invariance and 8×10^{-2} for transvection invariance in the C-band spectral range. A compact 1×4 splitter based on cascaded MMI coupler is proposed, showing a phase deviation less than 5.4° while maintaining a low-loss performance in C-band spectra.

Keywords: multimode interference coupler, optical unitary transformation, integrated photonics

PACS: 42.79.Sz, 42.82.–m, 42.82.Et **DOI:** 10.1088/1674-1056/ab5783

1. Introduction

Multimode interference (MMI) coupler is a kind of multi-port optical structure which performs the basic function of beam splitting and combining. The optical behaviors of light in MMI couplers have been described theoretically so far.[1–6] Many complex optical devices based on MMI couplers have been investigated such as optical couplers,[7–9] switches,[10–14] routers,[15,16] and hybrids.[17–21] The method of designing these devices was applied to a specific MMI coupler and the output amplitude and phase information corresponding to different input light were calculated.

In this paper, the optical unitary relation is proposed based on the transformation matrix for general nonoverlapping-image MMI couplers, which is important to the inverse design method for multi-port devices. Several inverse designs about MMI couplers are proposed based on the meta-materials.[22–24] However, the number of output port is less than three for these devices. The designs are also sophisticated because of the increasing difficulties for couplers with large output ports. For our proposed method, the only focus of inverse design is the optical inverse transformation matrix, which is essential for calculating the input light based on the output light with specific functions. When the ideal MMI couplers are lossless and liner, the inverse matrix is related to the property of unitarity. The mathematical proof of unitary transformation is presented, showing that the unitarity holds true for general nonoverlapping-image MMI couplers with any input and output ports. Taking 4×4 nonoverlapping-image MMI coupler based on the 220-nm silicon-on-insulator (SOI) for example,[25,26] the simulation based on the two-dimensional finite-difference time-domain (2D-FDTD) in C band spectrum shows that the unitarity is obtained within the deviation of 4×10^{-2} for the orthogonal invariance and 8×10^{-2} for the transvection invariance. To illustrate the inverse design method based on transformation matrix, a simplification for the input optical state of a 4×4 MMI coupler is investigated, which can be utilized in a cascaded structure to achieve a specific optical output state with equal power and phase difference.

2. Optical transformation matrix

The general nonoverlapping-image MMI coupler with N self-images is shown in Fig. 1. The light from any input port can be divided equally among N output ports. The self-image's phase information is

$$\varphi_{m,n} = \phi_1 - \frac{\pi}{2}(-1)^{m+n+N} + \frac{\pi}{4N}\times\left[m+n-m^2-n^2 + (-1)^{m+n+N}\left(2mn-m-n+\frac{1}{2}\right)\right], \quad (1)$$

where $\varphi_{m,n}$ denotes the phase change when light propagates from input port n to output port m. Then we can introduce the

*Project supported by the National Key Research and Development Program of China (Grant No. 2018YFB2200202) and the National Natural Science Foundation of China (Grant No. 61804148).

†Corresponding author. E-mail: lizhy@semi.ac.cn

© 2020 Chinese Physical Society and IOP Publishing Ltd

optical field transformation factor $T_{m,n}$. Assuming that the optical modes are the same for input ports and output ports, we use $\mathrm{e}^{\mathrm{i}\varphi_{m,n}}$ to represent the phase information and define $T_{m,n}$ as follows:

$$\begin{aligned} T_{m,n} &= \frac{1}{\sqrt{N}}\mathrm{e}^{\mathrm{i}\varphi_{m,n}} \\ &= \frac{1}{\sqrt{N}}\exp\left\{\mathrm{i}\left(\phi_1 - \frac{\pi}{2}(-1)^{m+n+N}\right.\right. \\ &\quad + \frac{\pi}{4N}\times\left[m+n-m^2-n^2\right. \\ &\quad \left.\left.\left. + (-1)^{m+n+N}\left(2mn-m-n+\frac{1}{2}\right)\right]\right)\right\}. \end{aligned} \tag{2}$$

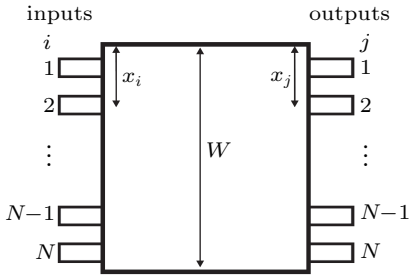


Fig. 1. Schematic view of general nonoverlapping-image MMI coupler.

3. Proof of optical unitary transformation

Unitarity is an important property of transformation matrix which requires that

$$T\cdot T^{\dagger} = I \quad \text{and} \quad I_{m,n} = \sum_{j=1}^{N} T_{m,j}\cdot T_{j,n}^{\dagger} = \delta_{m,n}, \tag{3}$$

where I is the unit matrix. To avoid confusion with imaginary unit i, we use j to represent the summing index and have

$$I_{m,n} = \sum_{j=1}^{N} T_{m,j}\cdot T_{j,n}^{\dagger} = \sum_{j=1}^{N} T_{m,j}\cdot T_{n,j}^{\dagger} = \frac{1}{N}\sum_{j=1}^{N}\mathrm{e}^{\mathrm{i}(\varphi_{m,j}-\varphi_{n,j})}. \tag{4}$$

For the case of $m = n$,

$$\begin{aligned} I_{m,n} &= \frac{1}{N}\sum_{j=1}^{N}\mathrm{e}^{\mathrm{i}(\varphi_{m,j}-\varphi_{n,j})} = \frac{1}{N}\sum_{j=1}^{N}\mathrm{e}^{\mathrm{i}(\varphi_{m,j}-\varphi_{m,j})} \\ &= \frac{1}{N}\sum_{j=1}^{N} 1 = 1, \end{aligned} \tag{5}$$

which shows that all of the elements on the main diagonal line of matrix I are equal to 1, which is a necessary condition for unitarity. For the case of $m \neq n$, using Eq. (3) we have

$$\begin{aligned} I_{m,n} &= \frac{1}{N}\sum_{j=1}^{N}\exp\left\{-\frac{\mathrm{i}\pi}{2}[(-1)^{m+j+N}-(-1)^{n+j+N}]\right. \\ &\quad + \frac{\mathrm{i}\pi}{4N}\left[m-n-m^2+n^2+(-1)^{m+j+N}\right. \\ &\quad \times\left(2mj-m-j+\frac{1}{2}\right) \\ &\quad \left.\left. -(-1)^{n+j+N}\left(2nj-n-j+\frac{1}{2}\right)\right]\right\}. \end{aligned} \tag{6}$$

Here, two cases are considered based on the parity of $m-n$. For generality, the following discussion is based on the assumption of $m > n$.

3.1. When $m - n$ is even

In the case where $m-n$ is even, $(-1)^{m+j+N}-(-1)^{n+j+N}$ must be zero. Define $m-n = 2a$ with integer a, then we will have

$$\begin{aligned} I_{m,n} &= \frac{1}{N}\sum_{j=1}^{N}\exp\left\{\frac{\mathrm{i}\pi}{4N}[2a-4am+4a^2\right. \\ &\quad \left.+(-1)^{m+j+N}(4aj-2a)]\right\}. \end{aligned} \tag{7}$$

It should be noted that the index j goes through 1 to N. Take the parity of $m+j+N$ into consideration and ignore the normalization factor of $1/N$ for brevity, then we will obtain

$$\begin{aligned} I_{m,n} &= \sum_{m+j+N=\text{even}}\exp\left[\frac{\mathrm{i}\pi a}{N}(a+j-m)\right] \\ &\quad + \sum_{m+j+N=\text{odd}}\exp\left[\frac{\mathrm{i}\pi a}{N}(a-j-m+1)\right]. \end{aligned} \tag{8}$$

Now $I_{m,n}$ can be written as the sum of two groups. When index j increases 2, phase term $\pi a\cdot(a+j-m)/N$ increases while phase term $\pi a\cdot(a-j-m+1)/N$ decreases and the phase variation is defined as $\Delta\varphi = 2\pi a/N$. It is noted that we cannot determine the parity of $m+j+N$ when $j=1$, so a further classification is essential.

For the case where $m+j+N$ is even when $j=1$, $I_{m,n}$ can be written as

$$\begin{aligned} I_{m,n} &= \sum_{j=1,3,5,\ldots}\exp\left[\frac{\mathrm{i}\pi a}{N}(a+j-m)\right] \\ &\quad + \sum_{j=2,4,6,\ldots}\exp\left[\frac{\mathrm{i}\pi a}{N}(a-j-m+1)\right]. \end{aligned} \tag{9}$$

Careful analysis shows that

$$\begin{aligned} &\frac{\pi a}{N}(a+j-m)\big|_{j=1} - \frac{\pi a}{N}(a-j-m+1)\big|_{j=2} \\ &= \frac{2\pi a}{N} = \Delta\varphi. \end{aligned} \tag{10}$$

So the minimum phase in sum sequence $\exp[\mathrm{i}\pi a/N(a+j-m)]$ (odd j) is larger than the maximum phase in sum sequence $\exp[\mathrm{i}\pi a/N(a-j-m+1)]$ (even j), with the difference of $\Delta\varphi = 2\pi a/N$. So we can combine the two parts into a whole sum sequence and rewrite it as $I_{m,n}$ in a general form:

$$\begin{aligned} I_{m,n} &= \frac{1}{N}\sum_{j=1}^{N}\mathrm{e}^{\mathrm{i}(j\Delta\varphi+\varphi_0)} = \frac{\mathrm{e}^{\mathrm{i}\varphi_0}}{N}\sum_{j=1}^{N}\mathrm{e}^{\mathrm{i}j\Delta\varphi} \\ &= \frac{\mathrm{e}^{\mathrm{i}\varphi_0}}{N}\frac{\mathrm{e}^{\mathrm{i}\Delta\varphi}(\mathrm{e}^{[(\mathrm{i}N)2\pi a/N]}-1)}{\mathrm{e}^{\mathrm{i}\Delta\varphi}-1} = 0. \end{aligned} \tag{11}$$

For the case where $m+j+N$ is odd, when $j=1$, we can make a similar discussion and arrive at $I_{m,n} = 0$.

3.2. When $m-n$ is odd

In this case where $m-n$ is odd, the sign of $(-1)^{m+j+N}$ and $(-1)^{n+j+N}$ must be different so $(-1)^{m+j+N}-(-1)^{n+j+N}=\pm 2$. Define $m-n=2a+1$ with integer a, then we will have

$$I_{m,n} = -\sum_{j=1}^{N}\exp\left\{\frac{\mathrm{i}\pi}{4N}[(2m-2a-2)(-1-2a) + (-1)^{m+j+N}(2j-1)(2\,m-2a-2)]\right\}. \quad (12)$$

Taking the parity of $m+j+N$ into consideration, we obtain

$$I_{m,n} = \sum_{m+j+N=\text{even}}\exp\left\{\frac{\mathrm{i}\pi}{N}[(m-a-1)(-1-a+j)]\right\} + \sum_{m+j+N=\text{odd}}\exp\left\{\frac{\mathrm{i}\pi}{N}[(m-a-1)(-a-j)]\right\}. \quad (13)$$

Both of the two parts in the above equation are also the sum of e-exponential terms and the phase satisfies the arithmetic progression with $\Delta\varphi=2\pi(m-a-1)/N$.

For the case where $m+j+N$ is even when $j=1$, we have

$$I_{m,n} = \sum_{j=1,3,5,\ldots}\exp\left\{\frac{\mathrm{i}\pi}{N}[(m-a-1)(-1-a+j)]\right\} + \sum_{j=2,4,6,\ldots}\exp\left\{\frac{\mathrm{i}\pi}{N}[(m-a-1)(-a-j)]\right\}, \quad (14)$$

$$\frac{\pi}{N}[(m-a-1)(-1-a+j)]\big|_{j=1} - \frac{\pi}{N}[(m-a-1)(-a-j)]\big|_{j=2} = \frac{2\pi(m-a-1)}{N}=\Delta\varphi. \quad (15)$$

So the minimum phase in sequence $\exp\{\mathrm{i}\pi/N[(m-a-1)(-1-a+j)]\}$ (odd j) is larger than the maximum phase in sequence $\exp\{\mathrm{i}\pi/N[(m-a-1)(-a-j)]\}$ (even j), with the difference $\Delta\varphi=2\pi(m-a-1)/N$. $I_{m,n}$ can still be written in a general form and proves to be

$$I_{m,n} = \frac{1}{N}\sum_{j=1}^{N}\mathrm{e}^{\mathrm{i}(j\Delta\varphi+\varphi_0)} = \frac{\mathrm{e}^{\mathrm{i}\varphi_0}}{N}\sum_{j=1}^{N}\mathrm{e}^{\mathrm{i}j\Delta\varphi} = \frac{\mathrm{e}^{\mathrm{i}\varphi_0}}{N}\frac{\mathrm{e}^{\mathrm{i}\Delta\varphi}\left(\mathrm{e}^{[(\mathrm{i}N)(2\pi a/N)]}-1\right)}{\mathrm{e}^{\mathrm{i}\Delta\varphi}-1}=0. \quad (16)$$

For the case where $m+j+N$ is odd when $j=1$, a similar discussion can be done and we can reach the conclusion that $I_{m,n}=0$. Now the elements of matrix I are all eqaual to 0 but for those on the main diagonal line, which is another necessary condition for unitarity. The elements on the main diagonal line of matrix I are all equal to1 and the others are 0. This is a direct proof of Eq. (4) so the optical field transformation matrix T has unitarity definitely.

4. Interpretation and simulation of unitarity

In matrix theory of quantum mechanics, a mechanical quantity operator can be written as a square matrix with unitarity and the wave function of a micro system's quantum state can be written as a column vector. The action of a mechanical quantity on a micro system can be realized as an action of the operator matrix on the column vector. The property of unitarity for the optical field transformation matrix T is proved, so the MMI coupler's interaction with input light can be explained as an acting process of the optical field transformation matrix on the column vector of light state.

Firstly, it is essential to introduce the column vector of light. The complex amplitude is used to represent the elements of the column vector. For example, when the input light with the complex amplitude E of electric field is incident from the first port, the column vector can be written as

$$\begin{bmatrix}E\\0\\\vdots\end{bmatrix}. \quad (17)$$

In this way, the whole column vector can be constructed by using the optical complex amplitude of each input port. Generally, for a 4×4 nonoverlapping multimode interference coupler, the input column vector In and the output column vector Out can be written as

$$In=\begin{bmatrix}a_1\\b_1\\c_1\\d_2\end{bmatrix} \quad \text{and} \quad Out=\begin{bmatrix}a_2\\b_2\\c_2\\d_2\end{bmatrix}. \quad (18)$$

Then the light propagation is equivalent to the mathematical transformation of $T\cdot In=Out$. In this way, the optical field transformation matrix T of any nonoverlapping multimode interference coupler can be calculated and matrix multiplication can be used to explain the light behaviors in these structures.

4.1. Orthogonal invariance relation

According to the unitary transformation, any two optical states which are orthogonal to each other should remain the orthogonal relation when they propagate to the output ports. Here is the simulation based on the 4×4 nonoverlapping-image MMI coupler. For two input light states $|A\rangle$ and $|B\rangle$, we have

$$|A\rangle=\begin{bmatrix}1\\\mathrm{i}\\-1\\-\mathrm{i}\end{bmatrix}, \quad |B\rangle=\begin{bmatrix}1\\-\mathrm{i}\\-1\\\mathrm{i}\end{bmatrix}, \quad \langle A\,|B\rangle=0. \quad (19)$$

The two input optical states are orthogonal to each other. Let the two states propagate through the coupler individually and the corresponding field profile is shown in Fig. 2, which is simulated by the Lumerical 2D-FDTD solutions.

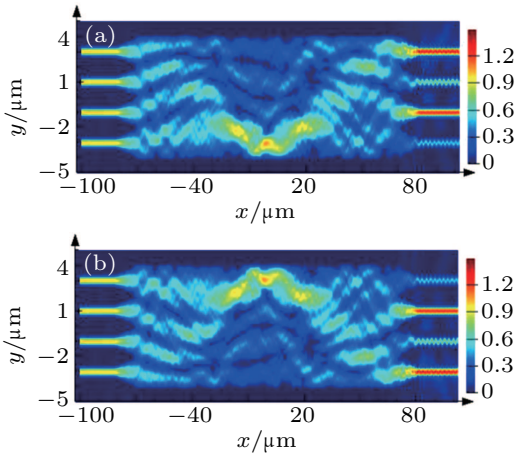


Fig. 2. Field profile for two optical input states: (a) $|A\rangle$ and (b) $|B\rangle$.

The device is based on SOI with 220-nm-thick top-silicon layer, and the optimized coupler's width and length are 142.8 μm and 8.0 μm respectively. The width of single mode waveguide is 500 nm with a lateral center spacing of 2 μm. For each output port, the light amplitude and phase information can be obtained by using the mode expansion monitors and frequency domain monitors, which can be used to construct the output light column vectors $|A_1\rangle$ and $|B_1\rangle$. The result of inner product $\langle A_1|\, B_1\rangle$ is shown in Fig. 3.

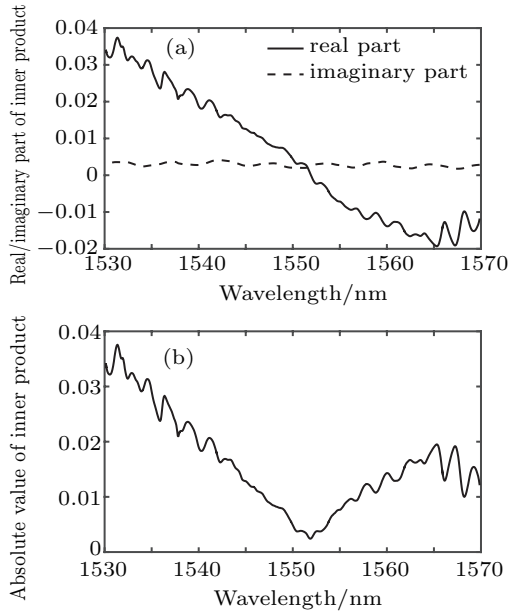


Fig. 3. (a) Real and imaginary parts of inner product for two output light states, and (b) absolute value of inner product for two output light states.

The calculated result shows that the inner product ranges from −0.0193 to 0.0374 for the real part and from 0.0018 to 0.0041 for the image part over C-band spectral range. At the edge of C band, the absolute value of inner product is larger than in the center of band due to the wavelength dependence of MMI couplers. The absolute value of inner product is less than 0.0376, which means that the orthogonal invariance relation is obtained within the deviation of 4×10^{-2} from 1530 nm to 1570 nm.

4.2. Transvection invariance relation

Based on the assumption of lossless condition, the conservation of energy should hold true for general nonoverlapping MMI coupler and this relation is a direct conclusion of unitarity. When the light is written as a column vector, the total energy is just the transvection between the light state vector and itself. Here the input light state is denoted as

$$|In\rangle = \frac{1}{\sqrt{15}} \begin{bmatrix} 1 \\ \sqrt{2} \\ 2 \\ 2\sqrt{2} \end{bmatrix}. \tag{20}$$

For this state, the power of four input ports satisfies the geometric progression of 1, 2, 4, 8, which is an important light state in optical applications such as signal sampling systems. When this state propagates through the same 4×4 MMI coupler as that mentioned in Subsection 4.1, the corresponding field profile is obtained and shown in Fig. 4.

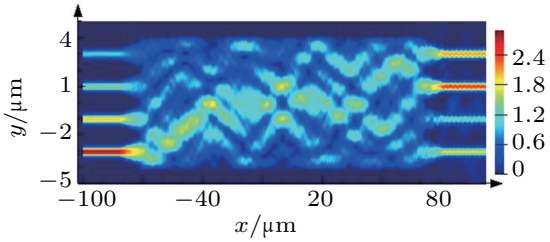


Fig. 4. Field profile for the optical input state $|In\rangle$.

The data of output amplitude and phase are collected by mode expansion monitors and frequency domain monitors, which can be used to construct the output light column vector $|Out\rangle$. The calculated output transvection of $\langle Out|\, Out\rangle$ is shown in Fig. 5.

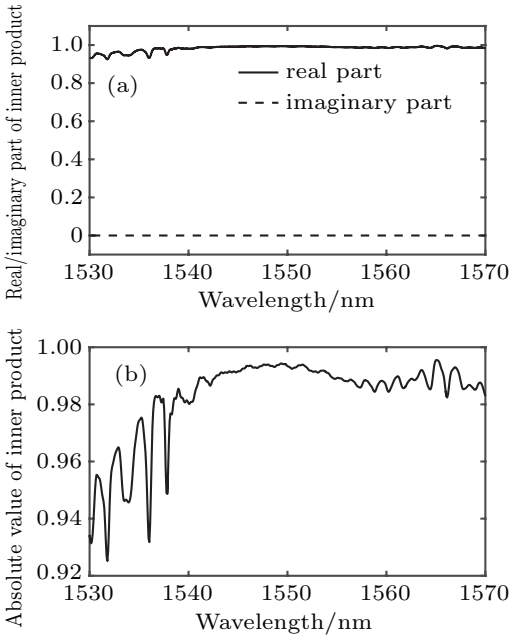


Fig. 5. (a) Real and imaginary parts of inner product for output inner product, (b) absolute value of output inner product.

The input light vector is normalized so the theoretical value of output inner product should be 1. According to the calculated results in the C-band spectral range, the real part of output inner product is in a range from 0.9252 to 0.9955 and the imaginary part is 0 for the whole range. The result of imaginary part is better than that of real part because the input inner product is just a real number in the complex plane and the argument is 0, which requires that the imaginary part is also 0. On the other hand, the physical significance of output inner product is power, which is actually a real number. For the real part, the deviation of value increases for the short wavelength region, which is caused by the mismatch of output images, causing output power to lose. The simulation accuracy is also a reason because some oscillations appear in the short wavelength region. Based on the above analysis, the relation of transvection is obtained within the deviation of 0.0748 in the C-band spectral range.

4.3. Inverse design for a 4-port output state

Here is an example of inverse design method based on the 4×4 MMI coupler mentioned in Subsection 4.1. The coupler is desired to achieve a 4-port output optical state with equal power and equal phase difference, which is important for the quadrature phase shift keying system.[27] This optical state can be written as

$$|Out\rangle = \begin{bmatrix} 1 \\ \mathrm{i} \\ -1 \\ -\mathrm{i} \end{bmatrix}. \tag{21}$$

For a common 4×4 nonoverlapping-image MMI coupler with minimum length L and optical transformation T to achieve such an optical state, the corresponding input state can be inversely calculated, which often requires that all of the four input ports be used. This kind of input state cannot simplify the problem, because the desired 4-port output state is changed into another 4-port input state. What actually makes sense is to achieve the desired state by requiring an input state to be less than 4 input ports, which is the instructive application of our inverse design method. We inversely calculate the input state of MMI couplers with different lengths (integer multiple of L) and find a simplified solution which only requires two input ports. The inverse calculation is expressed as

$$|In\rangle = [T^{\dagger}]^2\,|Out\rangle = \begin{bmatrix} 0.5-0.5\mathrm{i} \\ 0 \\ -0.5+0.5\mathrm{i} \\ 0 \end{bmatrix} = \begin{bmatrix} \frac{\sqrt{2}}{2}\mathrm{e}^{\mathrm{i}-\pi/4} \\ 0 \\ \frac{\sqrt{2}}{2}\mathrm{e}^{\mathrm{i}3\pi/4} \\ 0 \end{bmatrix}. \tag{22}$$

The length of MMI coupler is $2L_0$, so the inverse transformation matrix is $[T^{\dagger}]^2$. For the calculated input state column vector, the second and fourth element are both 0, which means only the first and third ports are needed. Furthermore, the amplitudes of the two required input light signals are the same and their phase angle has a difference of $-\pi$ (i.e., $-\pi/4-3\pi/4=-\pi$). This 2-port optical state can be exactly achieved by a small 1×2 MMI coupler when phase-shifting taper waveguides are incorporated for the two output ports. So the 1×2 MMI coupler can be set to be the first stage coupler which is connected by a 4×4 MMI coupler, constructing a cascaded 1×4 splitter which can achieve the desired output state. The diagram of the proposed cascaded splitter and simulated light profile are shown in Figs. 6(a) and 6(b), respectively.

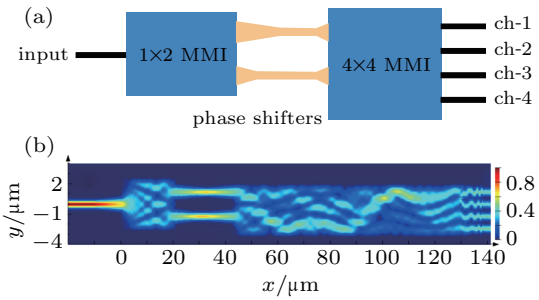


Fig. 6. (a) Diagram of 1×4 splitter based on cascaded MMI coupler, and (b) simulated light profile for 4-port output state with equal phase difference.

To achieve a device with more compact size, we re-optimize the 4×4 MMI coupler by an eigen-mode expansion (EME) method which is a three-dimensional optical solver. The input and output taper width are both set to be 1.2 μm. The optimal width and length of the 4×4 MMI coupler are 4.8 μm and 86.5 μm respectively. For the first stage 1×2 MMI coupler, the width is the same as that for the 4×4 MMI coupler while the length is 20.77 μm. To achieve a phase difference of π for the two output ports of 1×2 MMI coupler, the output taper waveguides are made to have a length difference of 3.1 μm, serving as a phase shifter between the two couplers. Figure 7 shows the simulated transmittance and phase characteristics of the proposed splitter.

As shown in Fig. 7(a), the 1×4 optical splitter exhibits uniform output power for the four channels and the power deviation is less than 0.38 dB. Because the theoretical normalized transmittance is 0.25 for each port, there is an intrinsic loss of 6 dB which is shown by a black horizontal dashed line. The average transmittance is about −6.37 dB for the four output channels, which means a slight insertion loss of device. Further calculation shows that the loss is less than 0.43 dB in a wavelength rane from 1530 nm to 1570 nm for all of the channels. Figure 7(b) shows the phase information of the proposed device which is an important characteristic for the inverse design method. Here the phase of channel-1 is set to be 0 serving as a reference value, because the relative phase between different channels is what essentially makes sense. The phase deviations for the other three channels within C-band

spectra are less than 5.0° (channel-2), 5.4° (channel-3), and 3.8° (channel-4) respectively, which shows that the proposed device based on inverse calculating method maintains a high phase-uniformity for the desired optical state.

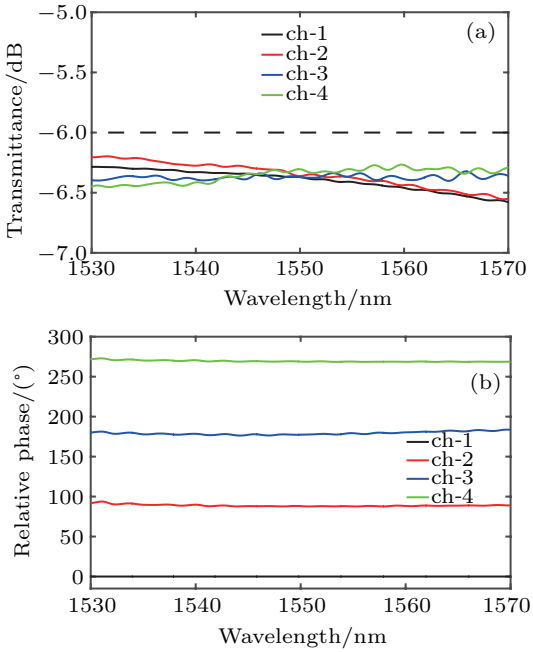


Fig. 7. (a) Normalized output power curves, with horizontal dashed line showing reference loss of −6 dB, and (b) phase characteristic of 1×4 splitter.

5. Conclusions and perspectives

In this work, the optical transformation matrix for the nonoverlapping MMI coupler along with the explanation of coupler's optical function is introduced. The unitarity for general nonoverlapping-image MMI couplers with any number of input/output ports is proved comprehensively. The optimized 4×4 MMI coupler based on 220-nm SOI exhibits an orthogonal invariance within a deviation of 4×10^{-2} and a transvection invariance within a deviation of 0.0748. The coupler's optical function is a unitary transformation when the light signals of different input/output ports are written as a column vector. The inverse design method can be utilized based on this view for any complex structures with cascaded MMI couplers. For calculating the input state of light, the amplitude and phase of any output light are free variables, which can be used to construct the output column vector multiplied by the transposed and complex conjugated matrix. Based on the inverse design method, a compact 1×4 optical splitter employing 2-stage cascaded MMI coupler is proposed which exhibits a power deviation less than 0.38 dB, an insertion loss less than 0.43 dB and a phase deviation less than 5.4° in C band. It is noted that the mentioned unitarity is not only a discrete transformation of matrix. Each discrete element of optical column vector can also represent a coefficient of continuous optical field along the lateral direction of MMI coupler, which shows that the inverse design method possesses practical applications in the design of complex optical field distribution.

References

[1] Heaton J M and Jenkins R M 1999 *IEEE Photon. Technol. Lett.* **11** 212
[2] Soldano L B and Pennings E C M 1995 *J. Lightwave Technol.* **13** 615
[3] Besse P A, Bachmann M, Nadler C and Melchior H 1995 *Opt. Quantum Electron.* **27** 909
[4] Ulrich R and Kamiya T 1978 *J. Opt. Soc. Am. A* **68** 583
[5] Paiam M R and MacDonald R I 1997 *Appl. Opt.* **36** 5097
[6] Bachmann M, Besse P A and Melchior H 1994 *Appl. Opt.* **33** 3905
[7] Soldano L B, Veerman F B, Smit M K, Verbeek B H, Dubost A H and Pennings E C M 1992 *J. Lightwave Technol.* **10** 1843
[8] Heaton J M, Jenkins R M, Wight D R, Parker J T, Birbeck J C H and Hilton K P 1992 *Appl. Phys. Lett.* **61** 1754
[9] Guo F, Lu D, Zhang R K, Wang H T, Wang W and Ji C 2016 *Chin. Phys. Lett.* **33** 024203
[10] Zhou J and Gallion P 2012 *J. Lightwave Technol.* **30** 15
[11] Mu S, Liu K, Wang S, Zhang C, Guan B and Zou D 2016 *Appl. Opt.* **55** 1795
[12] Cao-Dung T, Manh-Cuong N, Duy-Tien L and Trung-Thanh L 2016 *Opt. Switch. Netw.* **22** 129
[13] Mao Y Y, Sheng X Z, Wu C Q and Yu K L 2016 *Chin. Phys. Lett.* **33** 034204
[14] Mao Y Y, Sheng X Z, Wu C Q, Zhang T Y and Wang Y 2015 *Chin. Phys. Lett.* **32** 114204
[15] Crespo-Poveda A, Cantarero A and de Lima M M Jr 2016 *J. Opt. Soc. Am. B* **33** 81
[16] Huang J Z, Scarmozzino R and Osgood R M 1998 *IEEE Photon. Technol. Lett.* **10** 1292
[17] Uda R, Yamaguchi K, Takada K and Okamoto K 2018 *Appl. Opt.* **57** 3781
[18] Dong P, Xie C and Buhl L L 2014 *Opt. Express* **22** 2119
[19] Xue M, Pan S and Zhao Y 2014 *J. Lightwave Technol.* **32** 3317
[20] Zheng Z, Peng M, Zhou H, Chen M, Jiang L, Tan L, Dai X and Xiang Y 2018 *Opt. Commun.* **411** 21
[21] Deng X, Liu J, Jiao D D, Gao J, Zang Q, Xu G J, Dong R F, Liu T and Zhang S G 2016 *Chin. Phys. Lett.* **33** 114202
[22] Mak J C C, Sideris C, Jeong J, Hajimiri A and Poon J K S 2016 *Opt. Lett.* **41** 3868
[23] Piggott A Y, Lu J, Lagoudakis K G, Petykiewicz J, Babinec T M and Vuckovic J 2015 *Nat. Photon.* **9** 374
[24] Xu K, Liu L, Wen X, Sun W, Zhang N, Yi N, Sun S, Xiao S and Song Q 2017 *Opt. Lett.* **42** 855
[25] Li K L, An J M, Zhang J S, Wang Y, Wang L L, Li J G, Wu Y D, Yin X J and Hu X W 2016 *Chin. Phys. B* **25** 124209
[26] Xiao T H, Yu Y and Li Z Y 2017 *Acta Phys. Sin.* **66** 217802 (in Chinese)
[27] Su Y L, Feng H, Hu H, Wang W, Duan T, Wang Y S, Si J H, Xie X P, Yang H N and Huang X N 2019 *Chin. Phys. B* **28** 024216